e-Polymers **2003**, no. 039.

http://www.e-polymers.org
ISSN 1618-7229

Novel soluble blue emitting PPV-like polymers: synthesis and characterization

Jonas Gruber [1] *, *Rosamaria W. C. Li* [1], *Patricia Ponce* [1], *Adriano R. V. Benvenho* [2], *Regina M. Q. Mello* [3], *Ivo A. Hümmelgen* [2]

[1] Instituto de Química, Universidade de São Paulo, C.P. 26077, 05513-970 São Paulo, SP, Brazil; Fax +55 11 3815 5579; jogruber@iq.usp.br

[2] Departamento de Física, Universidade Federal do Paraná, C. P. 19044, 81531-990 Curitiba, PR, Brazil

[3] Departamento de Química, Universidade Federal do Paraná, C. P. 19081, 81531-990 Curitiba, PR, Brazil

(Received: June 10, 2003; published: August 7, 2003)

Abstract: We report on the electrochemical synthesis of two novel soluble PPV-like polymers, poly(2-decyloxy-4,4'-biphenylenevinylene), DOPBV, and poly(2-decylsulfonyl-4,4'-biphenylenevinylene), DSPBV, their spectroscopic and thermal characterization as well as their electrical properties. We also report on the use of sandwich devices Au/DOPBV/Al and Ni/DSPBV/Al to investigate the charge injection and transport characteristics, besides other important parameters such as the optical energy gap and the HOMO energy level, leading to an estimate of the ionization potential and electron affinity of these polymers.

Introduction

The past decades have witnessed unabated interest in the synthesis and characterization of poly(*p*-phenylenevinylene) (PPV) and its derivatives, offering new opportunities in the development of novel optoelectronic devices based on organic polymer films [1]. Although blue emitting organic materials have been reported [2], their stability and efficiency are still lower when compared to related red and green emitters. Therefore, novel blue emitting organic materials remain targets of synthetic interest.

In this contribution, we describe the synthesis and characterization of two novel PPV-like polymers, poly(2-decyloxy-4,4'-biphenylenevinylene), DOPBV, (Fig. 1, **1**), and poly(2-decylsulfonyl-4,4'-biphenylenevinylene), DSPBV (**2**), presenting alternating vinylene and biphenylene units substituted by long chain alkoxy (electron donating) or alkylsulfonyl (electron withdrawing) groups, which ensure high solubility in common organic solvents and, hence, allow formation of high quality thin films by spin-coating. We also describe the construction of sandwich devices Au/DOPBV/Al and Ni/DSPBV/Au to investigate the charge injection and transport characteristics, besides other important parameters such as optical energy gaps and HOMO levels, leading to estimates of the ionization potentials and electron affinities of these polymers.

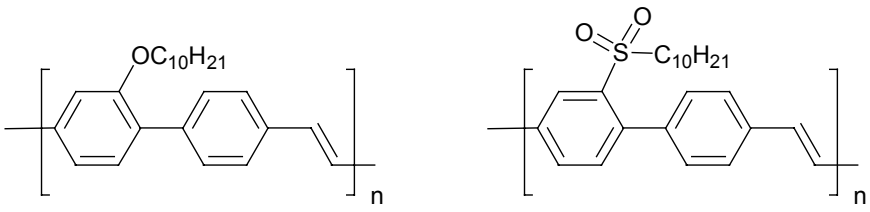

DOPBV (1) **DSPBV (2)**

Fig. 1. Structural formulae of DOPBV (**1**) and DSPBV (**2**)

Results and discussion

Synthetic aspects

As summarized in Scheme 1, the monomeric precursors **3** and **4** were synthesized by extensions of known literature methods starting from 2-bromo-5-methylphenol (**5**) [3] and 2-bromo-5-methylthiophenol (**6**) [4]. Preparation of biaryls **7** and **8** was successfully achieved *via* a palladium-catalyzed cross-coupling reaction (Suzuki reaction) [5] of commercial 4-methyl-phenylboronic acid with halides **9** and **10**, respectively. As far as we know, **3**, **4** and **7** - **10** are novel compounds. They have been fully characterized by ^{1}H NMR, FTIR and elemental analyses, which agreed with their expected structures.

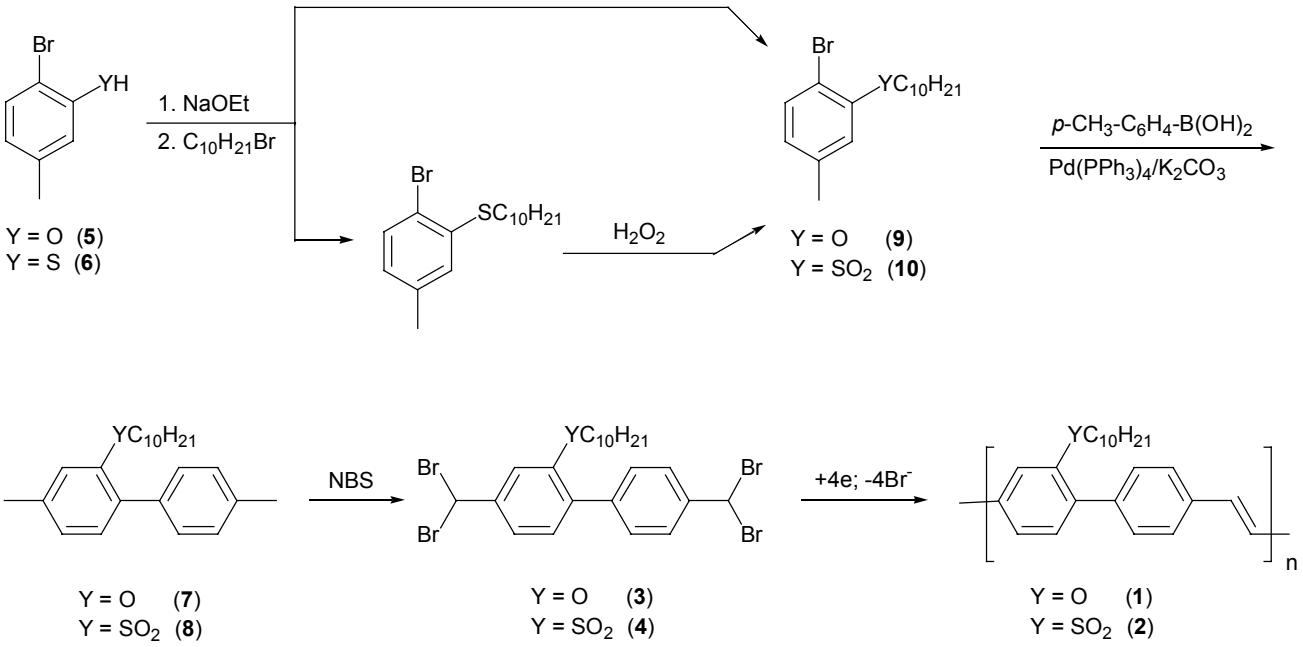

Scheme 1. Multistep synthesis of polymers **1** and **2**

The most negative of the reduction peaks observed in single-sweep cyclic voltammetry (CV) of compounds **3** (-2.1 V vs. standard calomel electrode, SCE) and **4** (-1.5 V vs. SCE) were used for the reduction potentials of controlled potential electrolyses [6] leading to polymers **1** and **2**. The *N*,*N*-dimethylformamide (DMF)-soluble polymer fractions (major products) were used for the characterization purposes that follow.

Characterization

Full spectroscopic data are given in the Exptl. part. Important observations include the IR absorptions at ≅ 960 cm^{-1}, which confirm the *trans*-alkene structure, strong bands at 1005 and 1274 cm^{-1} related to the C-O-C bonds of the substituent in polymer **1**, and bands at 1137 and 1307 cm^{-1} related to the SO_2 group of polymer **2**. The chemical shifts and integrations of the ^1H NMR signals are consistent with the conjugated backbone and the presence of long side-chains.

Thermal analyses, thermogravimetry (TG) (Fig. 2) and differential scanning calorimetry (DSC) (Fig. 3), revealed polymer **1** to be stable up to 250°C (2% weight loss). Above this temperature, it decomposes in two exothermic steps with inflection points at 340 and 543°C. Polymer **2** showed a similar behaviour except that there is an extra decomposition step starting at 120°C, which may correspond to sulfonyl-extrusion with loss of SO_2. Intriguing is the fact that the DSC curve didn't reveal any significant energy change in the temperature range between 25 and 250°C. Probably, there are several endothermic and exothermic processes involved (bond breaking, bond forming and SO_2 evaporation) that compensate energetically. Finally, for both polymers there was practically no residual weight above 600°C, suggesting total combustion of the specimens, and no melting or glass transition point could be observed.

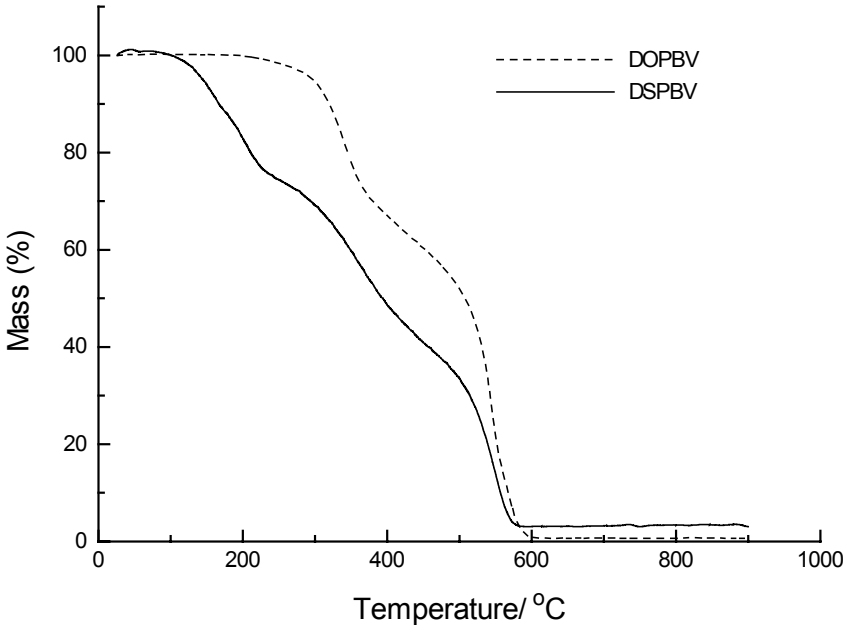

Fig. 2. TG curves of DOPBV and DSPBV, sample weights 3.31 and 1.27 mg, respectively. Dynamic air atmosphere, rate 10°C·min^{-1}

Examination by size exclusion chromatography (SEC) in tetrahydrofuran (THF) solution using polystyrene standards for comparison gave for DOPBV M_w = 53 000, M_n = 7000, M_w/M_n = 7.6 and n (degree of polymerization) = 159, and for DSPBV M_w = 3600, M_n = 950, M_w/M_n = 3.7 and n = 9.4. Although these results do not correspond to absolute values of molecular weight, they may be used to estimate relative values. Comparing the degrees of polymerization of both polymers one can note that, while polymer **1** is a true polymer, **2** is actually an oligomeric material. Probably, this difference may be owing to the electron withdrawing effect of the sulfonyl group,

facilitating the reduction of precursor **4**, and hence initiating a higher number of new chains, which at the end of the electrolyses become shorter in length, when compared to those originated from precursor **3**.

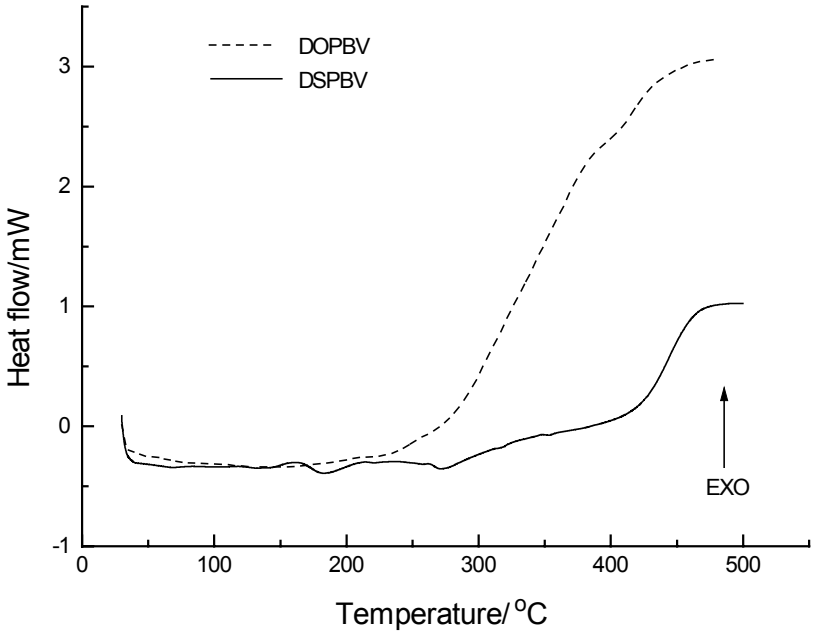

Fig. 3. DSC curves of DOPBV and DSPBV, sample weights 1.96 and 1.12 mg, respectively. Dynamic nitrogen atmosphere, rate 10°C·min^{-1}

Pressed discs of the polymers were exposed in a closed vessel to iodine vapour, for 24 h, and the electrical conductivity was measured immediately after removal from the vessel using the four-probe [7] and the two-probe [8] methods. The average conductivities were $(1.6 \pm 0.5) \cdot 10^{-5}$ S·cm^{-1} for DOPBV and $(4.7 \pm 0.5) \cdot 10^{-7}$ S·cm^{-1} for DSPBV, which are close to the values measured [9] for poly(2,2'-dimethoxy-4,4'-biphenylenevinylene) ($2 \cdot 10^{-5}$ S·cm^{-1}) and for poly(2,2'-dinitro-4,4'-biphenylenevinylene) ($3 \cdot 10^{-7}$ S·cm^{-1}) under the same experimental conditions. From these data it is reasonable to infer that for the above polymers, poly(biphenylenevinylene)s, the conductivity is much more related to the electronic nature of the substituent than to its length. Thus, the more electron withdrawing the group, the lower the conductivity.

The HOMO (highest occupied molecular orbital) level energies of DOPBV and DSPBV were estimated from CV experiments [10,11] based on a procedure reported by Micaroni et al. [11] Taking the oxidation onsets (Fig. 4) for DOPBV and DSPBV at ≈0.6 V and ≈0.5 V (vs. SCE), respectively, the ionization potentials were estimated as being ≈5.0 eV (DOPBV) and ≈4.9 eV (DSPBV).

Fig. 5 presents the absorption and photoluminescence spectra of DOPBV (0.3 μm thick) and DSPBV (0.2 μm thick) films, produced by casting from 5 mg·mL^{-1} (DOPBV) or 6 mg·mL^{-1} (DSPBV) solutions in $CHCl_3$ onto glass substrates. The calculated CIE (Comission Internationale de l'Eclairage) chromaticity coordinates of the photoluminescence (PL) spectrum are x = 0.145 and y = 0.128 (DOPBV) and x = 0.149 and y = 0.082 (DSPBV). The optical energy gaps E_g were determined following a procedure reported by Morita et al. [12] From analysis of the absorption edge and assuming direct transition, the gap can be calculated with help of the $(h\nu \cdot \eta)^2$ vs. $h\nu$ plot (where

η is the absorption coefficient, h is Planck's constant and ν the frequency). This procedure was applied, leading to E_g = 2.9 eV for DOPBV and E_g = 3.4 eV for DSPBV. Assuming the validity of Koopman's theorem [13], DOPBV presents an electron affinity of ≈2.1 eV and DSPBV of ≈1.5 eV. The maxima of the absorption and of the photoluminescence of both polymers are significantly displaced to shorter wavelengths, when compared to PPV. It is important to stress that the PL emission CIE coordinates of both polymers correspond to blue emission.

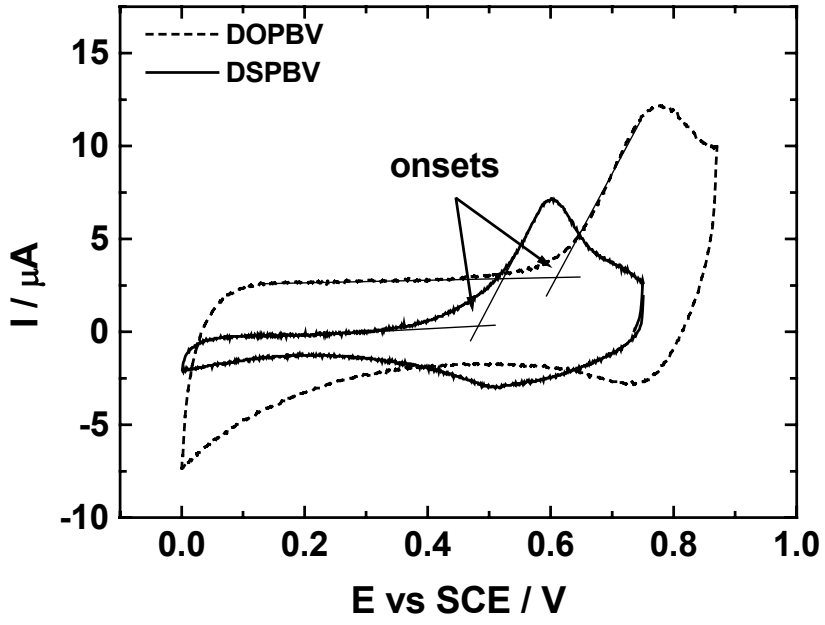

Fig. 4. Cyclic voltammogram (20 mV·s^{-1}) of DOPBV and DSPBV on Au substrate

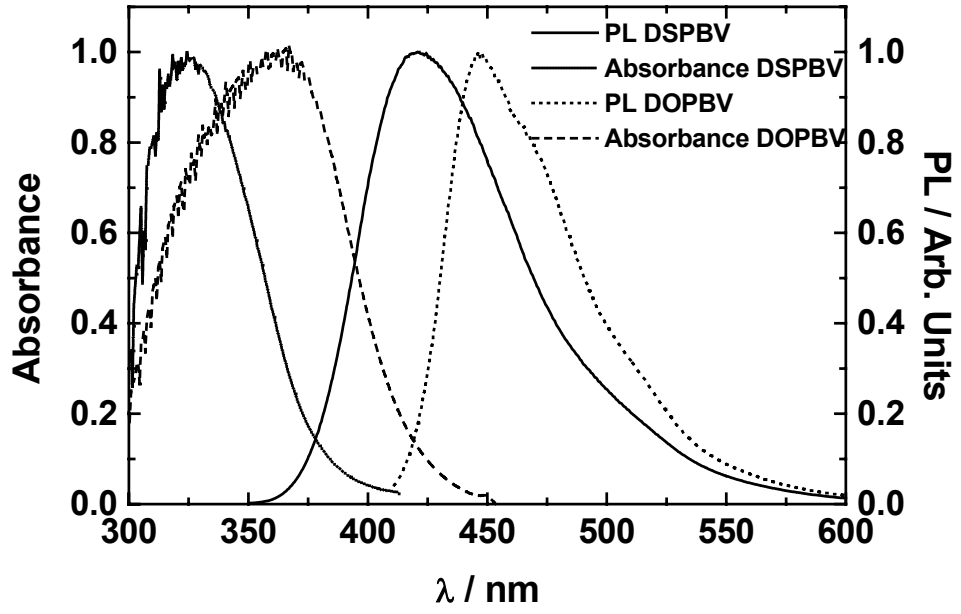

Fig. 5. Absorption and photoluminescence spectra of DOPBV and DSPBV films

A comparison of the optical gaps of DOPBV and DSPBV with those observed [9] for poly(2,2'-dimethoxy-4,4'-biphenylenevinylene) (3.2 eV) and poly(2,2'-dinitro-4,4'-

biphenylenevinylene) (3.7 eV) suggests a greater effective conjugation length, but less than the expected, most probably due to an increased degree of non-coplanarity between the biphenylene rings caused by steric hindrance of the long chain substituents. Again, the electronic nature of the substituent plays an important role for the E_g value.

The electrical characteristics of an Au/DOPBV/Al device can be seen in Fig. 6. Similarly to poly(4,4'-biphenylenevinylene) [14], the $I(V)$ behaviour can be described by Simmons expression for thermionic injection into low mobility materials [15], which predicts:

$$j = qN_v \mu F \exp\left(-\frac{\varphi}{\kappa T}\right)\exp\left(\frac{\beta F^{1/2}}{\kappa T}\right) \qquad (1)$$

where q is the elementary charge, N_v is the density of states accessible for charge transport, μ is the charge carrier mobility, φ is the energy barrier at the interface, κ is the Boltzmann constant, T is the absolute temperature, β is a constant and F is the electric field strength.

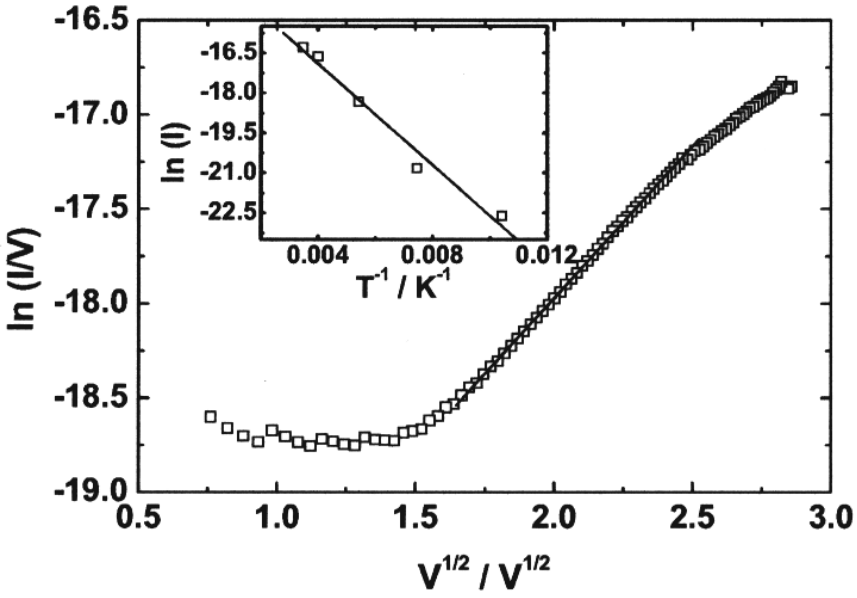

Fig. 6. $I(V)$ characteristics of a Au/DOPBV/Al device. Inset: temperature dependence of the current at V = 0.9 V

Eq. (1) predicts linear dependences between $\ln(j/V)$ and $V^{1/2}$, $\ln I$ and T^{-1}, and between $\ln(j \cdot d)$ and $d^{-1/2}$. These dependences were indeed observed (insets of Fig. 6 and Fig. 7, respectively), taking data of measurements done on several devices assembled with different film thickness. The data of Figs. 6 and 7 were used to determine the parameters μ and φ. The term $\left[\frac{\partial \ln jd}{\partial d^{-1/2}}\right]_{V=\text{constant}} = \frac{\beta V^{1/2}}{kT}$ can be determined using Fig. 7, and from the inset of Fig. 6 $\left[\frac{\partial \ln I}{\partial T^{-1}}\right]_{V=\text{constant}} = \frac{\beta d^{-1/2} V^{1/2} - \varphi}{k}$ can be calculated. Assuming [14] $N_v = 2.5 \cdot 10^{19}$ cm^{-3}, μ can then be obtained. The

analysis of the data leads to the following values for DOPBV: μ = (4.5 ± 0.7) · 10 $^{-11}$ cm^2·V^{-1}·s^{-1} and φ = 0.15 eV (Au/DOPBV interface). This mobility is nearly two orders of magnitude lower than the corresponding value for poly(4,4'-biphenylenevinyle) [14], which is 6 · 10 $^{-9}$ cm^2·V^{-1}·s^{-1}. The energy barrier at the gold interface is also lower than for poly(4,4'-biphenylenevinyle), where φ = 0.36 eV [14], indicating a strong mobility reduction due to lateral group introduction with a concomitant lowering of the ionization potential.

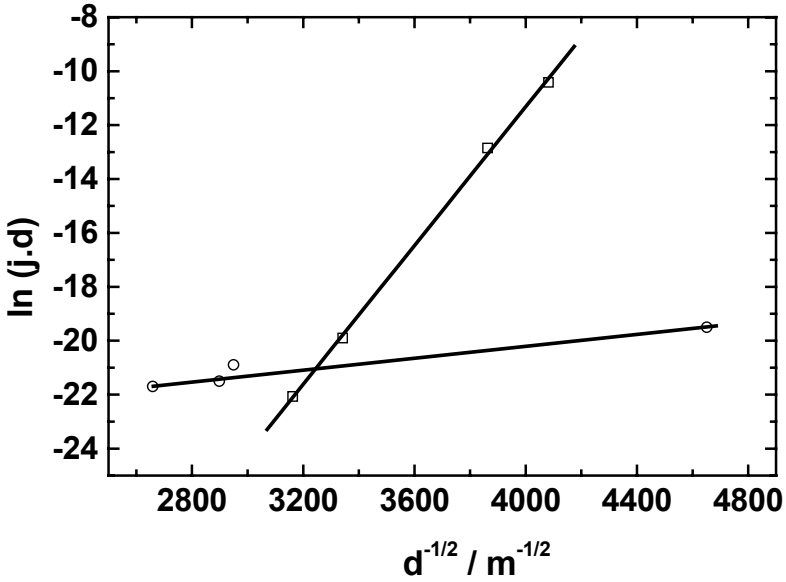

Fig. 7. Dependence of the current on DOPBV and DSPBV film thickness: in Au/ DOPBV/Al devices, with Au positively biased (circles), and in Ni/DSPBV/Al, with Ni positively biased (squares)

The *I*(*V*) characteristics of a Ni/DSPBV/Al device are presented in Fig. 8. It can be seen that the *I*(*V*) curve presents a hystheresis, the increasing-voltage current being lower than the decreasing-voltage one. This hystheresis suggests the presence of traps in the polymer. It can be seen from Fig. 9 that, for the decreasing-voltage *I*(*V*) curve, the dependence between ln(*j*/*V*) and $V^{1/2}$ is linear. Additionally, as presented in Fig. 7, there is a linear dependence between ln(*j* ·*d*) and $d^{-1/2}$ if current data of different devices (with different *d*) taken at constant *V*, always for decreasing voltage, are plotted. The temperature dependence of the current for these devices is presented in the inset of Fig. 9, indicating a linear dependence between ln *I* and T^{-1}. The dependence between ln(*j* ·*d*) and $d^{-1/2}$ is also linear (see Fig. 7). These observed dependences are consistent with those theoretically predicted by Eq. (1).

When there are traps in the polymer, the mobility μ is affected by the fraction of non-trapped charge θ, leading to an effective mobility $\mu_{\text{eff}} = \theta\mu = \frac{p}{p + p_t}\mu$, where *p* is the positive non-trapped charge carrier density and p_t is the positive trapped charge density. The hystheresis is attributed to the presence of deep traps in the polymer, which at low occupancy fraction (which corresponds to the condition θ < 1), significantly reduce charge mobility and, consequently, the device current. This is the case when the current density is progressively increased, at low injection conditions, leading to an *I*(*V*) curve that cannot be analytically described, due to the voltage-

dependent trap occupancy fraction. At higher voltages, i.e., high injection levels, the trap occupancy fraction approaches 1 ($p >> p_t \Rightarrow \theta \cong 1$) and remains at this condition as long as the charge injection is not excessively suppressed, which is observed at the decreasing-voltage segment of $I(V)$, except at low injection, $V < 0.8$ V.

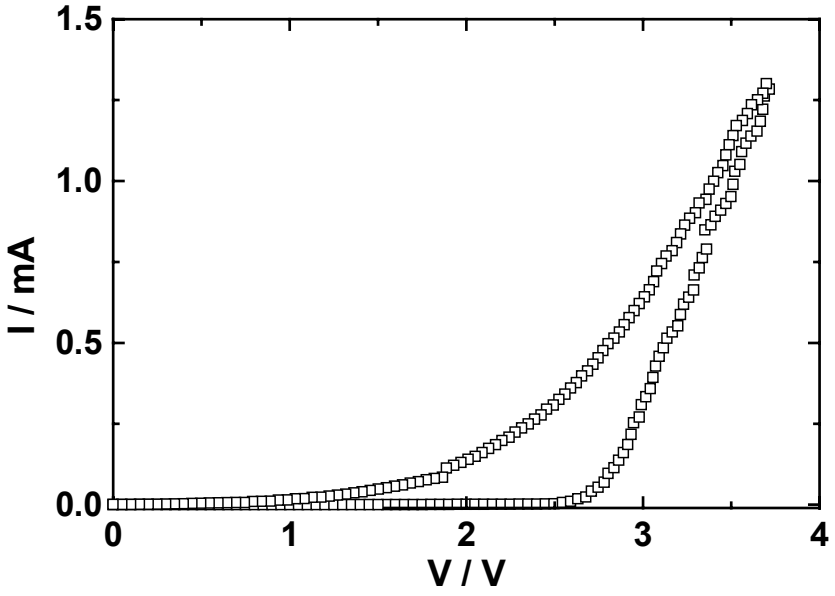

Fig. 8. $I(V)$ characteristics of a Ni/DSPBV/Al device (Ni positively biased). DSPBV film thickness: 60 nm

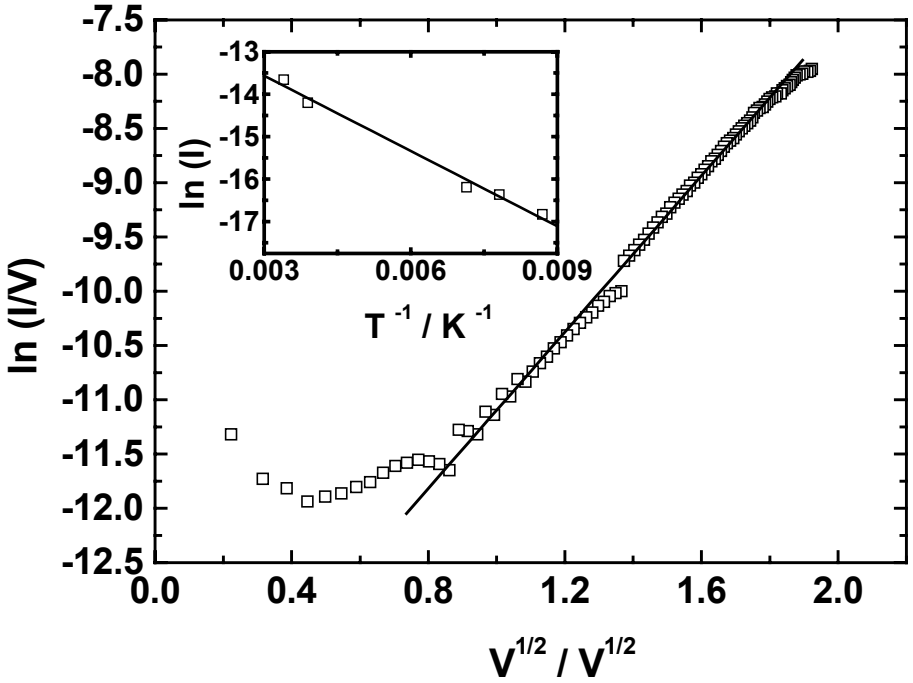

Fig. 9. ln(j/V) and $V^{1/2}$ plot for the decreasing-voltage $I(V)$ characteristics of Fig. 8

Using the same procedure as for DOPBV data analysis, assuming $N_v = 2.5 \cdot 10^{19}$ cm^{-3}, $\mu = (5.1 \pm 2.0) \cdot 10^{-8}$ cm^2·V^{-1}·s^{-1} and $\varphi = 0.14$ eV are calculated for DSPBV.

A similar value of φ in case of DOPBV and DSPBV devices would indeed be expected, since both polymers present almost the same estimated ionization potentials (estimated ionization potentials differing by approximately 0.1 eV) and the nominal work function values of the injection electrode materials, Ni and Au, are also similar.

In Tab. 1 we compare DSPBV energy gap and positive charge carrier mobility of the related polymers. PBV is interesting since it presents PL emission in the blue region of the spectrum, but presents processability constraints because of its low solubility in commonly available organic solvents. The introduction of the long aliphatic lateral segment in DOPBV significantly improves the solubility, permitting processing from solution and film preparation by spin coating or casting. Additionally, an increase in molecular weight associated to lateral segment introduction in polymers produced by electrochemical synthesis was observed, which improves film-forming properties. DOPBV has a lower positive charge carrier mobility, around two orders of magnitude, than PBV, and its absorption and emission characteristics are red shifted, both undesirable properties. In this sense, DSPBV presents an advantage, when compared to the formers: it has blue emission, is soluble, and its positive charge carrier mobility, after trap filling, is the highest among the polymers shown in Tab. 1.

Tab. 1. Comparison of E_g and μ for poly(4,4'-biphenylenevinylene) derivatives

Polymer structure	Acronym	μ/(cm^2·V^{-1}·s^{-1})	E_g /eV
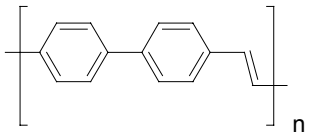	PBV [14]	$6 \cdot 10^{-9}$	3.3
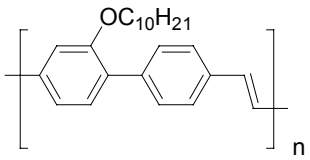	DOPBV	$5 \cdot 10^{-11}$	2.9
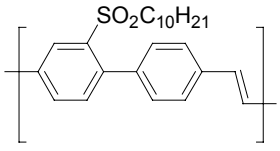	DSPBV	$5 \cdot 10^{-8}$	3.4

Experimental part

Physical measurements

Melting point data are uncorrected and were measured with a Dynamic Optics AHT microscope melting point apparatus.

^{1}H NMR FT spectra (200 MHz) were recorded on a Bruker AC-200 spectrometer using deuterated chloroform/tetramethylsilane (Aldrich) as solvent/reference.

FTIR spectra were recorded as a KBr disc or in solution ($CHCl_3$), on a Perkin-Elmer 1750 series grating. Only major or important absorptions are given.

Photoluminescence (PL) spectra were run on a Hitachi F4500 fluorescence spectrophotometer.

Cyclic voltammetric (CV) experiments were carried out using a USP electronics workshop-constructed triangular wave generator/potentiostat with a PAR RE0074 XY recorder. Controlled potential electrolysis experiments were carried out using a potentiostat/galvanostat with an electronic charge integrator constructed in our laboratory [16,17].

Differential scanning calorimetry (DSC) experiments were carried out on a Shimadzu DSC50 calorimeter with nitrogen as the purge gas, and thermogravimetry (TG) experiments on a Shimadzu TGA50 thermogravimeter with nitrogen or air as the purge gases. The heating rate was 10°C·min^{-1} in both cases.

Molecular weight determination was made by size exclusion chromatography (SEC) at a flow rate of 1 mL·min^{-1} in THF on a Shimadzu Class-LC10 HPLC equipped with three Supelco Progel columns (G5000 + G4000 + G3000). The molecular weight is reported relative to narrow-dispersity polystyrene standards (2500, 5000, 17 500, 30 000, 50 000, 95 800 and 184 200).

Elemental analyses were carried out on a Perkin Elmer Elemental Analyser 2400 CHN.

The electrical conductivities of doped polymer discs, prepared using a hydraulic press at a pressure of 1 ton·cm^{-2}, were measured using either a Signatone SP4-62.5-8.5-osmium tipped four-probe head or a two-probe head connected to an electrometer constructed in our laboratory [8].

Electrical measurements were performed using a Keithley 196 multimeter and a Keithley 230 programmable power supply, both connected via a GPIB interface to a Pentium III 1 GHz PC.

Syntheses

1-Bromo-2-decyloxy-4-methylbenzene (**9**)

0.645 g (28.1 mmol) of sodium was added to 15 mL of dry ethanol. After 30 min, a solution of 5.00 g (26.7 mmol) of 2-bromo-5-methylphenol (**5**) in 10 mL dry ethanol was added dropwise with stirring, followed by the addition of 9.33 g (42.2 mmol) of 1-bromodecane in 10 mL dry ethanol. The mixture was refluxed for 7 h, the solvent removed under reduced pressure, and 50 mL of water added. After extraction with dichloromethane (3 × 25 mL), washing with water (3 × 25 mL) and drying over anhydrous magnesium sulfate, the solvent was removed and the viscous liquid distilled under reduced pressure. 6.24 g (19.1 mmol; 72% yield) of the desired product were obtained; b.p. 150 - 152°C/0.15 mmHg.

^{1}H NMR ($CDCl_3$, ppm): δ = 7.37 (d, 1H, 6-Ar-*H*, *J* = 8 Hz); 6.69 (d, 1H, 3-Ar-*H*, *J* = 2 Hz); 6.62 (dd, 1H, 5-Ar-*H*, *J* = 8 Hz, *J* = 2 Hz); 3.97 (t, 2H, C*H*$_2$O, *J* = 7 Hz); 2.30 (s, 3H, C*H*$_3$); 1.82 (m, 2H, C*H*$_2$); 1.49 (m, 2H, C*H*$_2$); 1.27 (m, 12H, 6 × C*H*$_2$); 0.881 (t, 3H, C*H*$_3$, *J* = 7 Hz).

IR ($CHCl_3$): 3045 ($\nu_{arom.}$ C-H); 2925 and 2854 ($\nu_{sat.}$ C-H); 1586 and 1486 ($\nu_{arom.}$ C=C); 1469 and 1388 ($\delta_{sat.}$ C-H); 1284 ($\nu_{as.}$ C-O-C); 1042 ($\nu_{sym.}$ C-O-C); 843 ($\gamma_{arom.}$ 1 isol. C-H) and 801 cm^{-1} ($\gamma_{arom.}$ 2 adj. C-H).

$C_{17}H_{27}BrO$	Calc.	C	62.38	H	8.31
	Found	C	62.20	H	8.36

1-Bromo-2-decylsulfanyl-4-methylbenzene

1.67 g (72.6 mmol) of sodium was added to 40 mL of dry ethanol. After 30 min, a solution of 14.0 g (68.9 mmol) of 2-bromo-5-methylthiophenol (**6**) in 40 mL dry ethanol was added dropwise with stirring, followed by the addition of 16.8 g (76.0 mmol) of 1-bromodecane in 40 mL dry ethanol. The mixture was treated as above. 19.6 g (57.1 mmol; 83% yield) of the desired product were obtained; b.p. 160 - 166°C/0.25 mmHg.

^{1}H NMR ($CDCl_3$, ppm): δ = 7.39 (d, 1H, 6-Ar-*H*, *J* = 8 Hz); 7.02 (d, 1H, 3-Ar-*H*, *J* = 2 Hz); 6.81 (dd, 1H, 5-Ar-*H*, *J* = 8 Hz, *J* = 2 Hz); 2.91 (t, 2H, C*H*$_2$S, *J* = 8 Hz); 2.30 (s, 3H, C*H*$_3$); 1.66 (m, 2H, C*H*$_2$); 1.46 (m, 2H, C*H*$_2$); 1.27 (m, 12H, 6 × C*H*$_2$); 0.880 (t, 3H, C*H*$_3$, *J* = 6 Hz).

IR ($CHCl_3$): 3040 ($\nu_{arom.}$ C-H); 2952, 2924, 2853 ($\nu_{sat.}$ C-H); 1581 ($\nu_{arom.}$ C=C); 1455, 1378 ($\delta_{sat.}$ C-H); 867 ($\gamma_{arom.}$ 1 isol. C-H); 802 cm^{-1} ($\gamma_{arom.}$ 2 adj. C-H).

$C_{17}H_{27}BrS$	Calc.	C	59.47	H	7.93
	Found	C	59.67	H	7.83

1-Bromo-2-decylsulfonyl-4-methylbenzene (**10**)

15.5 g (45.1 mmol) of 1-bromo-2-decylsulfanyl-4-methylbenzene, 33 mL of glacial acetic acid and 17.2 mL of hydrogen peroxide 30% were mixed and refluxed for 2 h. After cooling to room temperature, water (300 mL) was added followed by a saturated aqueous sodium carbonate solution until neutral. The mixture was extracted with dichloromethane (3 × 30 mL) and the combined organic layer washed with water (2 × 50 mL) and dried over anhydrous magnesium sulfate. After solvent evaporation, 13.8 g (36.8 mmol; 82% yield) of white crystals were obtained, melting at 30 - 32°C.

^{1}H NMR ($CDCl_3$, ppm): δ = 7.96 (s, 1H, 3-Ar-*H*); 7.63 (d, 1H, 6-Ar-*H*, *J* = 8 Hz); 7.26 (d, 1H, 5-Ar-*H*, *J* = 8 Hz); 3.42 (t, 2H, C*H*$_2$SO$_2$, *J* = 8 Hz); 2.39 (s, 3H, C*H*$_3$); 1.69 (m, 2H, C*H*$_2$); 1.27 (m, 14H, 7 × C*H*$_2$); 0.872 (t, 3H, C*H*$_3$, *J* = 6 Hz).

IR (KBr): 3057 ($\nu_{arom.}$ C-H); 2923, 2854 ($\nu_{sat.}$ C-H); 1567 ($\nu_{arom.}$ C=C); 1461, 1379 ($\delta_{sat.}$ C-H); 1320 ($\nu_{as.}$ SO_2); 1147 ($\nu_{sim.}$ SO_2); 872 ($\gamma_{arom.}$ 1 isol. C-H); 820 cm^{-1} ($\gamma_{arom.}$ 2 adj. C-H).

$C_{17}H_{27}BrO_2S$	Calc.	C	54.40	H	7.25
	Found	C	54.28	H	6.96

2-Decyloxy-4,4'-dimethylbiphenyl (**7**)

Tetrakis(triphenylphosphine)palladium was prepared, shortly before use, following a literature procedure [18]. To a vigorously stirred solution, under nitrogen, of 1.00 g (7.36 mmol) 4-methyl-phenylboronic acid, 2.28 g (6.97 mmol) 1-bromo-2-decyloxy-4-methylbenzene (**9**), potassium carbonate solution (5.0 g in 40 mL water) and 40 mL 1,4-dioxane, 32.3 mg (0.280 mmol) of $Pd(PPh_3)_4$ were added and the reaction mixture was refluxed for 10 h. After cooling to room temperature, water (40 mL) was added; the mixture was extracted with dichloromethane (3 × 25 mL) and dried over anhydrous magnesium sulfate. The solvent was removed under reduced pressure and the crude product purified by column chromatography (alumina, 150 mesh, 58 Å, Aldrich) eluting with hexane. 1.97 g (5.82 mmol; 84% yield) of a viscous colourless liquid was obtained.

^{1}H NMR ($CDCl_3$, ppm): δ = 7.43 (d, 2H, 2',6'-Ar-*H*, *J* = 8 Hz); 7.21 (d, 2H, 3',5'-Ar-*H*, *J* = 8 Hz); 7.18 (d, 1H, 6-Ar-*H*, *J* = 8 Hz); 6.81 (dd, 1H, 5-Ar-*H*, *J* = 8 Hz, *J* = 1 Hz); 6.78 (s, 1H, 3-Ar-*H*); 3.93 (t, 2H, C*H*$_2$O, *J* = 7 Hz); 2.37 (s, 6H, 2 × C*H*$_3$); 1.71 (m, 2H, C*H*$_2$); 1.40 (m, 2H, C*H*$_2$); 1.26 (m, 12H, 6 × C*H*$_2$); 0.886 (t, 3H, C*H*$_3$, *J* = 7 Hz).

IR ($CHCl_3$): 3023 ($\nu_{arom.}$ C-H); 2924 and 2855 ($\nu_{sat.}$ C-H); 1611 and 1495 ($\nu_{arom.}$ C=C); 1465 and 1379 ($\delta_{sat.}$ C-H); 1275 ($\nu_{as.}$ C-O-C); 1171 ($\nu_{sym.}$ C-O-C); 825 ($\gamma_{arom.}$ 1 isol. C-H) and 804 cm^{-1} ($\gamma_{arom.}$ 2 adj. C-H).

$C_{24}H_{34}O$	Calc.	C	85.15	H	10.12
	Found	C	84.88	H	10.18

2-Decylsulfonyl-4,4'-dimethylbiphenyl (**8**)

0.399 g (2.93 mmol) 4-methyl-phenylboronic acid, 1.00 g (2.66 mmol) 1-bromo-2-decylsulfonyl-4-methylbenzene (**10**), potassium carbonate solution (2.5 g in 11 mL water), 18 mL 1,4-dioxane and 155 mg (0.134 mmol) of $Pd(PPh_3)_4$ were treated as above. The crude product was purified by column chromatography (alumina, 150 mesh, 58 Å, Aldrich) eluting with mixtures of 1:9 and then 1:4 of hexane/ethyl acetate. 0.942 g (2.44 mmol; 92% yield) of a viscous colourless liquid was obtained.

^{1}H NMR ($CDCl_3$, ppm): δ = 7.99 (s, 1H, 3-Ar-*H*); 7.42 (d, 1H, 5-Ar-*H*, *J* = 8 Hz); 7.33 (d, 2H, 2',6'-Ar-*H*, *J* = 8 Hz); 7.22 (d, 3H, 6,3',5'-Ar-*H*, *J* = 8 Hz); 2.59 (t, 2H, C*H*$_2$SO$_2$, *J* = 7 Hz); 2.47 (s, 3H, C*H*$_3$); 2.41 (s, 3H, C*H*$_3$); 1.42 (m, 2H, C*H*$_2$); 1.22 (m, 14H, 7 × C*H*$_2$); 0.873 (t, 3H, C*H*$_3$, *J* = 6 Hz).

IR ($CHCl_3$): 3053, 3025 ($\nu_{arom.}$ C-H); 2924, 2855 ($\nu_{sat.}$ C-H); 1607, 1480 ($\nu_{arom.}$ C=C); 1467, 1379 ($\delta_{sat.}$ C-H); 1306 ($\nu_{as.}$ SO_2); 1138 ($\nu_{sim.}$ SO_2); 877 ($\gamma_{arom.}$ 1 isol. C-H); 817 cm^{-1} ($\gamma_{arom.}$ 2 adj. C-H).

$C_{24}H_{34}O_2S$	Calc.	C	74.56	H	8.86
	Found	C	74.86	H	8.57

4,4'-Bis(dibromomethyl)-2-decyloxybiphenyl (**3**)

2-Decyloxy-4,4'-dimethylbiphenyl (**7**) (0.572 g; 1.69 mmol), *N*-bromosuccinimide (NBS) (1.27 g; 7.13 mmol) and dibenzoyl peroxide (60.0 mg) were added to dry carbon tetrachloride (20 ml) and heated to reflux for 4 h under VIS illumination (500 W halogen bulb), then cooled to room temperature. The insoluble succinimide was filtered off and then washed with chloroform. The combined filtrate was shaken with aqueous sodium chloride and then with water. After drying over anhydrous magnesium sulfate and solvent evaporation, the solid was recrystallized (ethyl acetate) and gave 0.541 g (0.827 mmol; 49% yield) of white crystals melting at 81 - 84°C.

^{1}H NMR ($CDCl_3$, ppm): δ = 7.60 (d, 2H, 2',6'-Ar-*H*, *J* = 8 Hz); 7.53 (d, 2H, 3',5'-Ar-*H*, *J* = 8 Hz); 7.28 (d, 1H, 6-Ar-*H*, *J* = 8 Hz); 7.21 (d, 1H, 3-Ar-*H*, *J* = 2 Hz); 7.15 (dd, 1H, 5-Ar-*H*, *J* = 8 Hz, *J* = 2 Hz); 6.70 (s, 1H, C*H*Br$_2$); 6.66 (s, 1H, C*H*Br$_2$); 4.03 (t, 2H, C*H*$_2$O, *J* = 7 Hz); 1.75 (m, 2H, C*H*$_2$); 1.27 (m, 14H, 7 × C*H*$_2$); 0.885 (t, 3H, C*H*$_3$, *J* = 7 Hz).

IR (KBr): 3012 ($\nu_{arom.}$ C-H); 2947, 2919 and 2851 ($\nu_{sat.}$ C-H); 1601 and 1472 ($\nu_{arom.}$ C=C); 1428 and 1396 ($\delta_{sat.}$ C-H); 1274 ($\nu_{as.}$ C-O-C); 1018 ($\nu_{sym.}$ C-O-C); 834 ($\gamma_{arom.}$ 1 isol. C-H) and 818 cm^{-1} ($\gamma_{arom.}$ 2 adj. C-H).

CV: -1.8 V vs. Ag/AgBr (-2.1 V vs. SCE).

$C_{24}H_{30}Br_4O$	Calc.	C	44.07	H	4.62
	Found	C	44.47	H	4.69

4,4'-Bis-dibromomethyl-2-decylsulfonylbiphenyl (**4**)

2-Decylsulfonyl-4,4'-dimethylbiphenyl (**8**) (0.574 g; 1.48 mmol), NBS (1.09 g; 6.12 mmol) and dibenzoyl peroxide (34.0 mg) were added to dry carbon tetrachloride (20 mL) and treated as above. The crude product was recrystallized from hexane and gave 0.527 g (0.751 mmol; 51% yield) of white crystals melting at 55 - 60°C.

^{1}H NMR ($CDCl_3$, ppm): δ = 8.32 (s, 1H, 3-Ar-*H*); 7.96 (d, 1H, 5-Ar-*H*, *J* = 8 Hz); 7.67 (d, 2H, 3',5'-Ar-*H*, *J* = 8 Hz); 7.47 (d, 3H, 6,2',6'-Ar-*H*, *J* = 8 Hz); 6.73 (s, 1H, C*H*Br_2); 6.71 (s, 1H, C*H*Br_2); 2.59 (t, 2H, CH_2SO_2, *J* = 7 Hz); 1.71 (m, 2H, CH_2); 1.22 (m, 14H, 7 $\times$ CH_2); 0.872 (t, 3H, CH_3, *J* = 6 Hz).

IR (KBr): 3056 ($\nu_{arom.}$ C-H); 2922, 2851 ($\nu_{sat.}$ C-H); 1605 ($\nu_{arom.}$ C=C); 1464, 1376 ($\delta_{sat.}$ C-H); 1312 ($\nu_{as.}$ SO_2); 1133 ($\nu_{sim.}$ SO_2); 894 ($\gamma_{arom.}$ 1 isol. C-H); 833 cm^{-1} ($\gamma_{arom.}$ 2 adj. C-H).

CV: -1.2 V vs. Ag/AgBr (-1.5 V vs. SCE).

$C_{24}H_{30}Br_4O_2S$	Calc.	C	41.05	H	4.31
	Found	C	41.36	H	4.37

Poly(2-decyloxy-4,4'-biphenylenevinylene), DOPBV (**1**)

Compound **3** (0.500 g; 0.764 mmol) was electrolysed at a stirred mercury pool cathode in Et_4NBr (0.1 mol·L^{-1}) DMF solution (50 mL), at -1.8 V (vs. Ag/AgBr) in a divided cell and a graphite anode. The cathode compartment was continually flushed with a slow stream of dry nitrogen. A yellow precipitate formed during electrolysis. After *c*. 4.2 F·mol^{-1} had passed, the cell current dropped close to the background value. The precipitate was filtered and washed several times with water to remove DMF and Et_4NBr, and dried *in vacuo*. Water was added to the filtrate and another crop of polymer was obtained (DMF-soluble fraction), which was also washed and dried. Yield: 41 mg (0.12 mmol; 16%) of insoluble fraction and 209 mg (0.626 mmol; 82%) of DMF-soluble fraction.

^{1}H NMR ($CDCl_3$, ppm): δ = 7.16-7.45 (br m, 7H, 6,2',3',5',6'-Ar-*H* and α,β-C*H*=C*H*); 6.78 (m, 2H, 3,5-Ar-*H*); 3.93 (m, 2H, CH_2O); 1.62 (m, 2H, CH_2); 1.26 (m, 14H, 7 $\times$ CH_2); 0.882 (m, 3H, CH_3).

IR (KBr): 3027 ($\nu_{arom.}$ C-H); 2922 and 2851 ($\nu_{sat.}$ C-H); 1602 and 1492 ($\nu_{arom.}$ C=C); 1466 and 1393 ($\delta_{sat.}$ C-H); 1274 ($\nu_{as.}$ C-O-C); 1005 ($\nu_{sym.}$ C-O-C); 963 cm^{-1} ($\nu_{sym.}$ *trans* C*H*=C*H*).

Poly(2-decylsulfonyl-4,4'-biphenylenevinylene), DSPBV (**2**)

Compound **4** (0.500 g; 0.712 mmol) was electrolysed as above at -1.2 V (vs. Ag/AgBr). Yield: 10 mg (0.026 mmol; 4%) of insoluble fraction and 162 mg (0.424 mmol; 60%) of DMF-soluble fraction.

^{1}H NMR ($CDCl_3$, ppm): δ = 8.16 (s, 1H, 3-Ar-*H*); 7.45 (m, 3H, 5,3',5'-Ar-*H*); 7.24 (m, 5H, 6,2',6'-Ar-*H* and α,β-C*H*=C*H*); 2.47 (m, 2H, CH_2SO_2); 1.25 (m, 16H, 8 $\times$ CH_2); 0.882 (m, 3H, CH_3).

IR (KBr): 3053 and 3028 ($\nu_{arom.}$ C-H); 2924 and 2853 ($\nu_{sat.}$ C-H); 1605 and 1476 ($\nu_{arom.}$ C=C); 1377 ($\delta_{sat.}$ C-H); 1307 ($\nu_{as.}$ SO_2); 1137 ($\nu_{sim.}$ SO_2); 967 cm^{-1} ($\nu_{sym.}$ C*H*=C*H trans*).

Polymer film preparation and characterization

Au/DOPBV/Al (or Ni/DSPBV/Al) devices were prepared onto glass in sandwich structure. Firstly, Au (or Ni) was evaporated onto glass, then DOPBV (or DSPBV) was spin-coated from chloroform solution (5 $mg \cdot mL^{-1}$ in the case of DOPBV and 6 $mg \cdot mL^{-1}$ in the case of DSPBV) and, finally, Al was evaporated onto the DOPBV (or DSPBV) film. The film thickness was determined using a surface profiler.

After device preparation and during electrical measurements the films were kept under nitrogen atmosphere. *I*(*V*) curves were obtained as reported earlier [14,19]. The applied voltage was changed stepwise (0.1 V/step) at a rate of 0.1 $V \cdot s^{-1}$.

Cyclic voltammograms were obtained with DOPBV films produced from a 3:10 w/w tetrabutylammonium tetrafluoroborate (TBATFB)/DOPBV solution in chloroform (5 $mg \cdot mL^{-1}$), spin-coated onto Au electrode. During the measurements the films were immersed in a 0.1 $mol \cdot L^{-1}$ TBATFB/acetonitrile solution, under nitrogen atmosphere. An Ag wire was used as a quasi-reference electrode. Its electrochemical potential was assumed to be 0.01 V vs. SCE [10], so that for practical purposes it can be considered the same as of SCE. In case of DSPBV, the cyclic voltammograms were obtained with DSPBV films produced from a 1:5 w/w $LiClO_4$/DSPBV solution in chloroform (6 $mg \cdot mL^{-1}$), spin-coated onto Au electrode. During the measurements the films were immersed in a 0.1 $mol \cdot L^{-1}$ $LiClO_4$/acetonitrile solution, under nitrogen atmosphere. An Ag wire was used as a quasi-reference electrode.

Conclusions

The cathodic elimination reaction of 4,4'-bis(dibromomethyl)-2-decyloxybiphenyl (**3**) and of 4,4'-bis(dibromomethyl)-2-decylsulfonylbiphenyl (**4**) led to the corresponding polymers, DOPBV (**1**) and DSPBV (**2**), under mild conditions and with yields above 60%. Both polymers showed good solubility in common organic solvents, such as DMF, THF and chloroform, and an average molecular weight of 53 000 for DOPBV and 3600 for DSPBV. From UV-VIS and CV experiments it was possible to estimate the ionization potential (≈5.0 eV), electron affinity (≈2.1 eV) and optical band gap (≈2.9 eV) of DOPBV. Charge transport measurements were used to estimate its positive charge carrier mobility ($4.5 \cdot 10^{-11}$ $cm^2 \cdot V^{-1} \cdot s^{-1}$). The same experiments using DSPBV permitted to estimate the corresponding quantities for that polymer: ionization potential (≈4.9 eV), electron affinity (≈1.5 eV), optical band gap (≈3.4 eV) and positive charge carrier mobility ($5.1 \cdot 10^{-8}$ $cm^2 \cdot V^{-1} \cdot s^{-1}$).

Acknowledgement: The authors would like to thank FAPESP, PADCT/CNPq, CAPES and CNPq for their financial supports, and Dr. Jivaldo R. Matos and Adriano A. A. S. Araujo for the thermal analyses.

[1] Gruber, J.; Li, R. W. C.; Hümmelgen, I. A.; "*Synthesis, properties, and applications of poly(p-phenylenevinylene)s*", in '*Handbook of Advanced Electronic and Photonic*

Materials and Devices', vol. *8*, Nalwa, H. S., editor; Academic Press, San Diego **2001**, chapter 4, pp. 163-184.

[2] Kim, D. Y.; Cho, H. N.; Kim, C. Y.; *Prog. Polym. Sci.* **2000**, *25*, 1089.

[3] Huston, R. C.; Peterson, W. J.; *J. Am. Chem. Soc.* **1933**, *55*, 3879.

[4] Dixit, K. N.; Joland, S. D.; Rajagopal, S.; *Monatsh. Chem*. **1963**, *94*, 414.

[5] Miyaura, N.; Suzuki, A.; *Chem. Rev*. **1995**, *95*, 2457.

[6] Utley, J. H. P.; Gao, Y.; Gruber, J.; Zhang, Y.; Muñoz-Escalona, A.; *J. Mater. Chem*. **1995**, *5*, 1837.

[7] Van der Pauw, L. J.; *Philips Res. Rep*. **1985**, *13*, 1.

[8] Gruber, J.; Santana, H.; Gruber, I.; Gazotti, W.; *J. Chem. Educ*. **1997**, *74*, 418.

[9] Gruber, J.; Li, R. W. C.; *J. Mater. Chem*. **1999**, *9*, 1461.

[10] Li, Y.; Cao, Y.; Gao, J.; Wang, D.; Yu, G.; Heeger, A. J.; *Synth. Met*. **1999**, *99*, 243.

[11] Micaroni, L.; Nart, F. C.; Hümmelgen, I. A.; *J. Solid State Electrochem*. **2002**, *7*, 55.

[12] Morita, S.; Akashi, T.; Fujii, A.; Yoshida, M.; Ohmori, Y.; Yoshimoto, K.; Kawai, T.; Zakhidrov, A. A.; Lee, S. B.; Yoshino, K.; *Synth. Met.* **1995**, *69*, 433.

[13] Levine, I. N.; "*Quantum Chemistry*", Prentice Hall, New York **1991**, p. 275.

[14] Ma, D.; Hümmelgen, I. A.; Li, R. W. C.; Gruber, J.; *J. Phys. D, Appl. Phys*. **2000**, *33*, 1376.

[15] Simmons, J.; *Phys. Rev. Lett*. **1965**, *25*, 967.

[16] Gruber, J.; Pardini, V. L.; Viertler, H.; *Quim. Nova* **1992**, *15*, 83.

[17] Gruber, J.; Pardini, V. L.; Viertler, H.; Gruber, I.; *Anal. Instrum*. **1992**, *20*, 155.

[18] Barbiéri, R. S.; Massabni, A. C.; Bellato, C. R.; *Quim. Nova* **1991**, *14*, 212.

[19] Ma, D.; Hümmelgen, I. A.; Jing, X.; Hong, Z.; Wang, L.; Zhao, X.; Wang, F.; *J. Appl. Phys.* **2000**, *87*, 312.